CHEMISTRY
A EUROPEAN JOURNAL

Rhodium-Catalyzed Dehydrocoupling of Fluorinated Phosphine–Borane Adducts: Synthesis, Characterization, and Properties of Cyclic and Polymeric Phosphinoboranes with Electron-Withdrawing Substituents at Phosphorus

Timothy J. Clark,[a] José M. Rodezno,[a] Scott B. Clendenning,[a, b] Stephane Aouba,[c] Peter M. Brodersen,[d] Alan J. Lough,[a] Harry E. Ruda,[c] and Ian Manners*[a]

Dedicated to Professor Peter Paetzold on the occasion of his 70th birthday

Abstract: The dehydrocoupling of the fluorinated secondary phosphine–borane adduct $R_2PH{\cdot}BH_3$ (R = *p*-$CF_3C_6H_4$) at 60 °C is catalyzed by the rhodium complex [{Rh(μ-Cl)(1,5-cod)}$_2$] to give the four-membered chain $R_2PH\text{-}BH_2\text{-}R_2P\text{-}BH_3$. A mixture of the cyclic trimer $[R_2P\text{-}BH_2]_3$ and tetramer $[R_2P\text{-}BH_2]_4$ was obtained from the same reaction at a more elevated temperature of 100 °C. The analogous rhodium-catalyzed dehydrocoupling of the primary phosphine–borane adduct $RPH_2{\cdot}BH_3$ at 60 °C gave the high molecular weight polyphosphinoborane polymer $[RPH\text{-}BH_2]_n$ (M_w = 56170, PDI = 1.67). The molecular weight was investigated by gel permeation chromatography and the compound characterized by multinuclear NMR spectroscopy. Interestingly, the electron-withdrawing fluorinated aryl substituents have an important influence on the reactivity as the dehydrocoupling process occurred efficiently at the mildest temperatures observed for phosphine–borane adducts to date. Thin films of polymeric $[RPH\text{-}BH_2]_n$ (R = *p*-$CF_3C_6H_4$) have also been shown to function as effective negative-tone resists towards electron beam (e-beam) lithography (EBL). The resultant patterned bars were characterized by scanning electron microscopy (SEM), atomic force microscopy (AFM) and time-of-flight secondary ion mass spectrometry (TOF-SIMS).

Keywords: boranes · fluorinated ligands · lithography · phosphanes · polymers

Introduction

The discovery of new and efficient synthetic methods for the formation of bonds between main group elements is of considerable interest for the general development of molecular and polymeric main group chemistry.[1–3] Transition metal catalyzed reactions are of widespread importance in organic chemistry whereas their use in preparative inorganic chemistry is much less explored. However, examples of the use of transition metal catalyzed dehydrocoupling reactions for the preparation of a variety of homo- and heteronuclear bonds between main group elements have been demonstrated beginning with the use of titanocene complexes to convert primary silanes to polysilanes in 1986.[4] New classes of inorganic macromolecules such as polystannanes[5] have been generated via catalytic dehydrocoupling methods while several examples of P–P,[6] B–Si,[7] Sn–Te,[8] Si–P,[9] Si–N[10] and Si–O[11] bond-forming reactions have also been reported.[12] As part of our continuing program to develop novel extended structures based on main group elements,[13] we have studied the late transition metal (e.g. rhodium) cata-

[a] T. J. Clark, J. M. Rodezno, Dr. S. B. Clendenning, Dr. A. J. Lough, Prof. I. Manners
Department of Chemistry, University of Toronto
80 St. George Street
Toronto, ON, M5S 3H6 (Canada)
Fax: (+1) 416-978-2450
E-mail: imanners@chem.utoronto.ca

[b] Dr. S. B. Clendenning
Current Address: Intel Corporation
RA3-252, 2513 NW 229th Ave.
Hillsboro, OR 97124 (USA)

[c] Dr. S. Aouba, Prof. H. E. Ruda
Centre for Advanced Nanotechnology
University of Toronto, 170 College Street
Toronto, ON, M5S 3E3 (Canada)

[d] Dr. P. M. Brodersen
Surface Interface Ontario
Department of Chemical Engineering and Applied Chemistry
University of Toronto, 200 College Street
Toronto, ON, M5S 3E5 (Canada)

DOI: 10.1002/chem.200401296

lyzed formation of phosphorus–boron bonds, and its application to the dehydrocoupling of phosphine–borane adducts of the type $R_2PH{\cdot}BH_3$ and $RPH_2{\cdot}BH_3$. This has resulted in the development of new synthetic routes to phosphine–borane rings, chains and macromolecules.[14–17] In addition, the catalytic dehydrocoupling approach has been extended to amine–borane adducts to yield cyclic products with B–N skeletons.[18]

The electronic nature of the substituents at phosphorus in phosphine–borane adducts might be expected to significantly influence both the rate of dehydrocoupling and the polymer properties. The observation that the catalytic dehydrocoupling of $PhPH_2{\cdot}BH_3$ and $Ph_2PH{\cdot}BH_3$ is more facile compared with that of iBuPH$_2{\cdot}$BH$_3$ and iBu$_2$PH$\cdot$BH$_3$[16] as well as tBu$_2$PH$\cdot$BH$_3$[19] is likely associated with differences in the polarity of the P–H bonds. The strong (+)-inductive effect of the alkyl group attached to phosphorus is expected to decrease the polarity of the P-H functionality, which in turn, would be anticipated to render the bond less reactive for catalytic dehydrocoupling with $B^{\delta+}$–$H^{\delta-}$ bonds.[16] Conversely, the presence of electron withdrawing substituents on phosphorus would be expected to make metal-catalyzed dehydrocoupling reactions more favourable. Furthermore, the presence of the fluorinated substituents would represent a significant new structural variation for polyphosphinoboranes as this would be expected to introduce additional useful properties.[20] With these considerations in mind, in this paper we report our work on the synthesis and catalytic dehydrocoupling behaviour of the fluoroaryl-substituted phosphine–borane adducts (p-$CF_3C_6H_4)_2PH{\cdot}BH_3$ and (p-$CF_3C_6H_4)PH_2{\cdot}BH_3$. Furthermore, we describe preliminary investigations into the use of polymeric fluorinated phosphinoboranes as resists towards electron beam (e-beam) lithography (EBL).

Results and Discussion

Synthesis and characterization of secondary and primary phosphine-borane adducts 1 and 2: We have previously shown that primary phosphine–borane adducts $RPH_2{\cdot}BH_3$ (R = Ph, iBu, p-nBuC$_6$H$_4$, p-dodecylC$_6$H$_4$) undergo rhodium-catalyzed dehydrocoupling between 90–130 °C to yield moderate to high molecular weight polyphosphinoboranes.[15,16] The synthesis of these polymers was most effectively achieved using rhodium (pre)catalysts [{Rh(μ-Cl)(1,5-cod)}$_2$], [Rh(cod)$_2$]OTf, anhydrous $RhCl_3$, or $RhCl_3{\cdot}xH_2O$ (ca. 1–2 mol % Rh). Previously, it was shown by ^{31}P and ^{11}B NMR spectroscopy that in the absence of Rh catalyst, the reactions are very slow and yield poorly defined oligomeric materials that appear to have branched structures.[15] To investigate whether aryl-substituted monomers bearing electronegative groups are indeed more reactive than those previously studied, we synthesized and investigated the *para*-substituted phosphine–borane adducts (p-$CF_3C_6H_4)_2PH{\cdot}BH_3$ **1** and (p-$CF_3C_6H_4)PH_2{\cdot}BH_3$ **2**. The secondary phosphine–borane adduct **1** was isolated as a colorless oil in 72 % overall yield in four steps from PCl_3 by using a protection–deprotection sequence (Scheme 1).

The primary phosphine–borane adduct **2** was prepared in an analogous manner to **1** and was isolated as a white solid in 64 % overall yield via the procedure shown in Scheme 2.

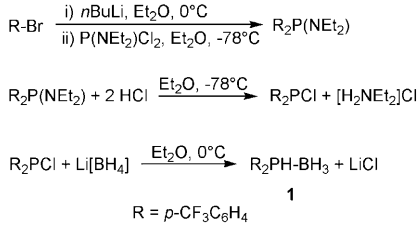

Scheme 1.

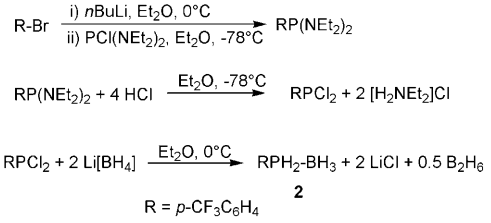

Scheme 2.

Characterization of **1** and **2** was achieved by ^{1}H, ^{31}P, ^{13}C, ^{19}F and ^{11}B NMR spectroscopy and mass spectrometry, which afforded spectra completely consistent with the assigned structures. For example, the ^{31}P NMR spectrum of **1** displayed a doublet ($^1J_{PH}$ = 386 Hz) due to coupling to one PH proton while **2** exhibited a triplet ($^1J_{PH}$ = 370 Hz) due to the presence of the PH_2 moiety when the ^{1}H coupled spectrum was recorded. The ^{1}H NMR spectrum of **2** reflected the greater acidity of the PH_2 protons relative to those in $PhPH_2{\cdot}BH_3$ in accordance with the electron withdrawing trifluoromethyl functionalities on the phenyl ring of **2**. The signal for the PH_2 protons in $PhPH_2{\cdot}BH_3$ was observed at δ 5.51 ppm[21] while the signal for **2** was detected further downfield at δ 5.60 ppm.

Single crystals of **1** suitable for X-ray analysis were obtained by cooling the neat compound to −30 °C. The geometry around phosphorus and boron is approximately tetrahedral, and their substituents are oriented in a staggered conformation (Figure 1). The smallest angle at phosphorus is 101.1(9)° (H(1P)-P(1)-C(1)), and the largest is 115.6(9)° (H(1P)-P(1)-B)1)) while the angles at boron range from 103.8(13) to 115(2)°. The P–B bond length of 1.917(2) Å in **1** is typical for a P–B single bond (1.90–2.00 Å)[22] and no intermolecular hydrogen bonding between P–H and B–H substituents was observed.

Single crystals of **2** suitable for X-ray analysis were also obtained by cooling the neat phosphine–borane adduct (to −35 °C) over several days (Figure 2a and b). Compound **2** was also found to possess a staggered geometry around the

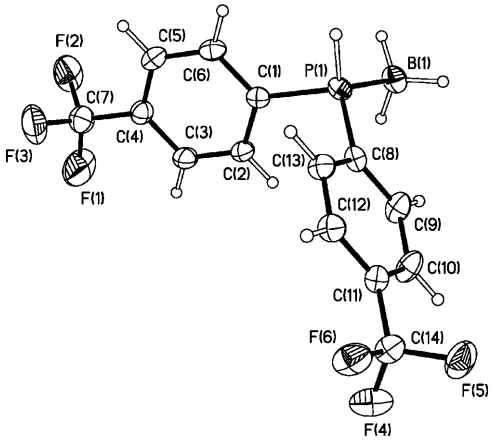

Figure 1. Molecular structure (p-$CF_3C_6H_4)_2PH$-BH_3 (**1**). Selected bond lengths [Å] and angles [°]: P(1)–B(1) 1.917(2), P(1)–H(1P) 1.37(2), B(1)–H(1B) 1.12(2), B(1)–H(2B) 1.07(3), B(1)–H(3B) 1.09(3); H(1P)-P(1)-B(1) 115.6(9), H(1B)-B(1)-P(1) 103.8(13), H(2B)-B(1)-P(1) 104.5(15), H(3B)-B(1)-P(1) 105.8(15).

tetrahedral phosphorus and boron atoms with a P–B bond length of 1.900(3) Å. In a similar manner to the molecular structure of $PhPH_2{\cdot}BH_3$,[15] close intermolecular P-$H^{\delta+}$···$^{\delta-}$H-B contacts were found between two molecules of **2** creating a centrosymmetric dimer. The closest contacts were found to be 2.308 Å, however, these distances are underestimated due to the systematic error in determining hydrogen positions in X-ray structures. After standardization with a value of 1.21 Å used for B–H bonds (established by neutron diffraction)[23] and 1.40 Å for P–H bonds (determined by microwave spectroscopy),[24] the H···H distances were found to be 2.230 Å. This value is significantly shorter than the sum of the van der Waals radii for two hydrogen atoms (2.4 Å) suggesting an attractive P-$H^{\delta+}$···$^{\delta-}$H-B interaction exists as a result of the oppositely charged hydrogen atoms. Furthermore, the P-H···H angle (165.86(2.37)°) is more linear relative to the B-H···H angle (134(3)°), which is also observed for most compounds with an N-$H^{\delta+}$···$^{\delta-}$H-B interaction.[23]

Rhodium-catalyzed dehydrocoupling of the secondary phosphine–borane adduct (p-$CF_3C_6H_4)_2PH{\cdot}BH_3$ (1)—Synthesis and characterization of (p-$CF_3C_6H_4)_2PH$-BH_2-(p-$CF_3C_6H_4)_2P$-BH_3 (3): The dehydrocoupling of **1** was found to be catalyzed by the rhodium complex [{Rh(μ-Cl)(1,5-cod)}$_2$] at 60 °C over 15 h affording the linear dimer (p-$CF_3C_6H_4)_2PH$-BH_2-(p-$CF_3C_6H_4)_2P$-BH_3 (**3**) (Scheme 3) in 69 % yield. Pure **3** was obtained by recrystallization from diethyl ether as a colorless, air- and moisture-stable crystalline solid.

The $^{31}P\{^1H\}$ NMR spectrum of **3** in $CDCl_3$ showed two broad resonances at δ −2.1 [(p-$CF_3C_6H_4)_2PH$] and at δ −14.7 ppm [(p-$CF_3C_6H_4)_2P$]. The resonance at δ −2.1 ppm was further split into a doublet in the ^1H coupled ^{31}P NMR spectrum ($^1J_{PH}$ = 437 Hz). The $^{11}B\{^1H\}$ NMR spectrum of **3** also showed two broad lines centered at δ −33.6 ppm [BH_2] and δ −37.8 ppm [BH_3]. The ^1H NMR spectrum of **3** showed a doublet of multiplets centered at δ 6.98 ppm ($^1J_{PH}$ = 425 Hz, PH proton) and two sets of broad resonances assigned to the BH_2 and BH_3 protons centered around 1.00 and 2.40 ppm, respectively. When compared with Ph_2PH-BH_2-PPh_2-BH_3, obtained from heating neat $Ph_2PH{\cdot}BH_3$ at 90 °C with a Rh (pre)catalyst, we observed almost indistinguishable ^1H NMR spectroscopic data.[15]

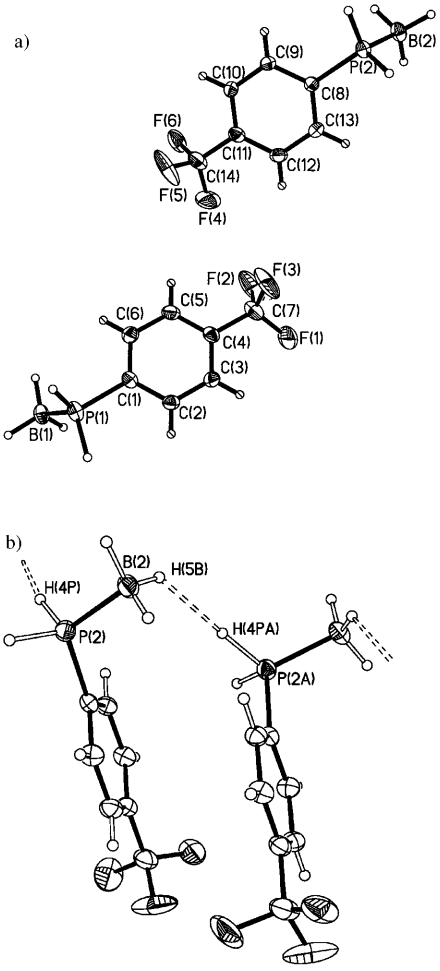

Figure 2. a) Molecular structure p-$CF_3C_6H_4PH_2$-BH_3 (**2**) and its symmetry-related neighbour. Selected bond lengths [Å] and angles [°]: P(1)–B(1) 1.900(3), P(1)–H(1P) 1.29(3), P(1)–H(2P) 1.42(3), B(1)–H(1B) 1.11(3), B(1)–H(2B) 1.16(3), B(1)–H(3B) 1.11(4); H(1P)-P(1)-B(1) 111.8(12), H(2P)-P(1)-B(1) 112.5(11), H(1B)-B(1)-P(1) 108.4(14), H(2B)-B(1)-P(1) 108.2(16), H(3B)-B(1)-P(1) 98.9(19); b) molecular structure p-$CF_3C_6H_4PH_2$-BH_3 (**2**) and its symmetry-related neighbour (symmetry code "A": x, 0.5−y, 0.5+z), showing weak intermolecular H···H interactions; selected bond angles [°]: B(2)-H(5B)-H(4PA) 134(3), P(2A)-H(4PA)-H(5B) 165.9(2.4).

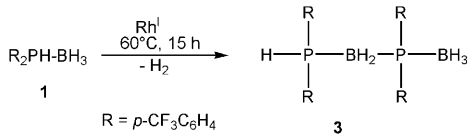

Scheme 3.

Single-crystal X-ray analysis of compound **3** confirmed the assigned structure based on a PBPB chain (Figure 3). The geometries around B(1), B(2), P(1) and P(2) are approximately tetrahedral, with bond angles varying from 104.1(18) to 112.4(16)°, 106.8(18) to 113(3)°, 103.3(12) to 115.46(18)° and 102.83(15) to 112.95(19)°, respectively. All three P–B distances are in the single bond range with P(1)–B(1) 1.916(4), P(2)–B(1) 1.935(4) and P(2)–B(2) 1.929(4) Å.

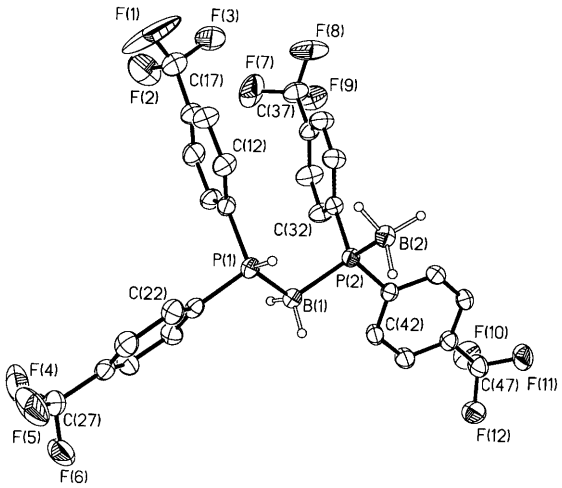

Figure 3. Molecular structure $(p\text{-}CF_3C_6H_4)_2PH\text{-}BH_2\text{-}(p\text{-}CF_3C_6H_4)_2P\text{-}BH_3$ (**3**). Selected bond lengths [Å] and angles [°]: P(1)–B(1) 1.916(4), P(2)–B(1) 1.935(4), P(2)–B(2) 1.929(4), P(1)–H(1P) 1.30(3), B(2)-P(2)-B(1) 112.95(19), H(1P)-P(1)-B(1) 114.9(12), P(1)-B(1)-P(2) 108.7(2). Hydrogen atoms attached to phenyl rings are omitted.

Interestingly, no transformation of **1** into **3** occurs when the compound is heated in the melt in the absence of Rh catalyst under the same conditions (60 °C, 15 h) verifying the crucial role the catalyst plays in the dehydrocoupling reaction at this temperature. Moreover, the catalytic reaction conditions employed to form $Ph_2PH\text{-}BH_2\text{-}PPh_2\text{-}BH_3$ from $Ph_2PH{\cdot}BH_3$ (90 °C, 15 h) are more forcing compared to those required to form **3**. This significant difference in reaction temperature can likely be attributed to the presence of the electron-withdrawing trifluoromethyl substituents on the phenyl rings of the phosphorus atom of **1** compared with $Ph_2PH\text{-}BH_3$ as this is the only variance in composition between the two compounds.

Synthesis and characterization of $[(p\text{-}CF_3C_6H_4)_2P\text{-}BH_2]_3$ (4a) and $[(p\text{-}CF_3C_6H_4)_2P\text{-}BH_2]_4$ (4b): When neat **1** and ≈ 1–2 mol % $[\{Rh(\mu\text{-}Cl)(1,5\text{-}cod)\}_2]$ were heated at 100 °C for 15 h, the linear compound **3** was no longer observed as the reaction product. Instead a mixture of cyclic trimer **4a** and cyclic tetramer **4b** was isolated (Scheme 4).

Multinuclear NMR studies of **4a** and **4b** revealed that there are virtually no differences in their ^{31}P and ^{11}B NMR spectra. For example, the ^{31}P NMR spectrum of the mixture revealed a broad signal centered at δ −18.5 ppm, which is similar to that of $[Ph_2P\text{-}BH_2]_3$ and $[Ph_2P\text{-}BH_2]_4$ centered at δ

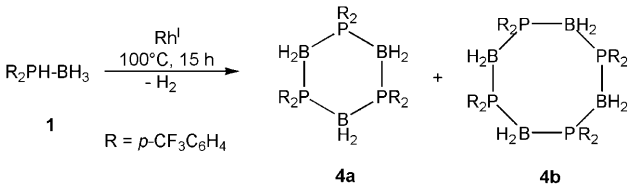

Scheme 4.

−18.2 ppm.[15] However, the ^1H NMR spectrum in $[D_8]$THF showed two sets of aromatic protons that were assigned to **4a** and **4b**, respectively, in the ratio of 4:1.

It was possible to isolate pure samples of the cyclic tetramer **4b**, which is significantly less soluble in dichloromethane than trimer **4a**. Although we have been unable to isolate single crystals of **4a** for X-ray analysis from diethyl ether and THF solutions, single crystals of **4b** were obtained from the slow evaporation of a THF solution. From these crystals, an X-ray diffraction study was carried out which proved the eight-membered ring structure of **4b** (Figure 4).

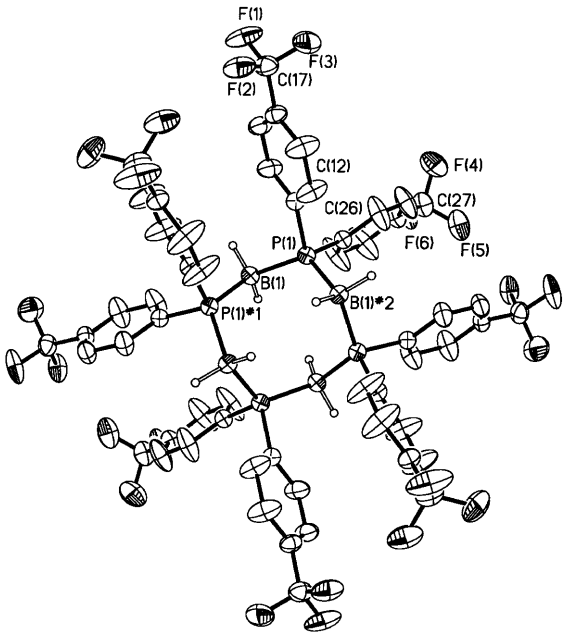

Figure 4. Molecular structure $[(p\text{-}CF_3C_6H_4)_2P\text{-}BH_2]_4$ (**4b**). Selected bond lengths [Å] and angles [°]: P(1)–B(1) 1.956(5), P(1)–B(1)#1 1.933(5), P(1)#2–B(1) 1.933(5), B(1)#1-P(1)-B(1) 120.5(3), P(1)#2-B(1)-P(1) 112.9(2). Hydrogen atoms attached to phenyl rings are omitted.

In an analogous manner to the structure of $[Ph_2P\text{-}BH_2]_4$, molecules of **4b** were found to exist in a boat–boat conformation and possess similar bond lengths and bond angles to those found in the former compound.[15] The P–B single bond lengths are 1.933(5) and 1.956(5) Å. The B-P-B and the P-B-P bond angles are 120.5(3) and 112.9(2)°, respectively. The B-P-B bond angle deviates from the expected tetrahedral value (ca. 109°) possibly due to steric interactions between the aryl groups.

Heating **1** alone at 100 °C for 15 h in the absence of Rh catalyst does not lead to the ring systems **4a** and **4b**. However, approximately 50 % of the monomer does undergo dehydrocoupling at this temperature to afford **3**. The reaction conditions employed to prepare $[Ph_2P\text{-}BH_2]_x$ ($x = 3$, 4) involved heating $Ph_2PH{\cdot}BH_3$ with Rh^I (pre)catalysts to 120 °C.[15] In comparison, it is likely that the decrease in dehydrocoupling temperature by 20 °C reflects the increased acidity and reactivity of the P-H functionality in **1** compared with that in $Ph_2PH{\cdot}BH_3$.

Rhodium-catalyzed dehydrocoupling of the primary phosphine-borane adduct (p-$CF_3C_6H_4$)$PH_2{\cdot}BH_3$ (2): Synthesis and characterization of polyphosphinoborane [(p-$CF_3C_6H_4$)PH-BH_2]$_n$ (5): Upon treatment of neat **2** with a catalytic amount (2.5 mol %) of $[\{Rh(\mu\text{-}Cl)(1,5\text{-}cod)\}_2]$ at 60 °C for 9 h, dehydrocoupling was observed with the reaction mixture gradually becoming viscous after several hours. Dissolution of the orange residue in THF and subsequent precipitation into pentane gave light brown fibers, which were identified as the polyphosphinoborane **5** (Scheme 5).

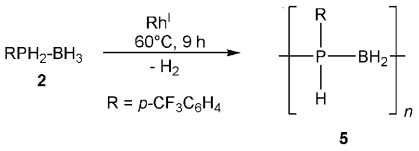

Scheme 5.

The ^{31}P NMR spectrum of **5** showed three resonances that resemble a 1:2:1 triplet at δ −46.9 ppm, which are in close proximity to the resonance of monomer **2** (δ −48.3 ppm). The appearance of three peaks is consistent with the formation of an atactic polymer with resolution of the triad structure. Thus, the possible triad configurations in **5** involve four distinct tacticity environments composed of two successive dyads, namely *mm*, *mr*, *rm*, and *rr*, where *m* and *r* are the *meso* (adjacent units of the same configuration) and racemic (adjacent units of opposite configuration) forms, respectively. Since *mr* and *rm* configurations are mirror images, they are indistinguishable by NMR and this leads to the expected statistical distribution of 1:2:1 in the ^{31}P NMR spectrum.[25] The resonance centered at δ −46.9 ppm split into a broad doublet ($^1J_{PH} = 354$ Hz) when the ^1H coupled ^{31}P NMR spectrum was recorded, which supported the presence of a single hydrogen substituent at the phosphorus.

The ^1H NMR spectrum of **5** is also consistent with the assigned structure and contains broad peaks for the aromatic protons (δ 7.9–6.9) and the BH_2 protons (δ 1–2), as well as a broad doublet centered at δ 4.42 for the PH group ($^1J_{PH} =$ 354 Hz). The ^{11}B NMR spectrum of **5** showed a single broad resonance at δ −34.3, which is consistent with a four-coordinate boron center attached to two phosphorus atoms.[26] The ^{19}F NMR resonance for **5** at δ −62.5 ppm differs slightly from that of monomer **2** (δ −63.7 ppm). As previously reported for other polyphosphinoboranes,[15,16] polymer **5** is also air- and moisture-stable in the solid state.

We have investigated the molecular weight of polymer **5** through gel permeation chromatography (GPC) experiments. Previous studies on solutions of high molecular weight polymers $[RPH\text{-}BH_2]_n$ (R = Ph, *i*Bu) in THF by using GPC for molecular weight characterization were found to be problematic due to facile aggregation and/or adsorption of the polymer chains to the GPC columns. This behavior is not surprising as low angle light scattering studies showed that THF is a θ solvent under these conditions.[15,16] However, in contrast, GPC analysis of other polyphosphinoboranes (R = p-*n*BuC_6H_4, p-dodecylC_6H_4) in THF revealed M_w values that were in fairly good agreement with estimates provided by hydrodynamic radius data obtained from dynamic light scattering.[16] Initial GPC studies of **5** were conducted in THF but consistently indicated long elution times consistent with column adsorption effects. However, increasing the ionic strength of the eluent by addition of $[Bu_4N]Br$[27] was found to lead to well-defined GPC peaks which showed that the material was of high molecular weight (M_w = 56170, PDI = 1.67). We presume that the use of the 3 mM salt solution lowers the affinity of polymeric **5** for the column.[27]

Due to the step-growth nature of the polycondensation reaction used to form polyphosphinoboranes, very high conversion (>99 %) of the phosphine–borane adducts is required to obtain high molecular weights. Unfortunately, there was a general tendency for the neat reaction mixture to become increasingly viscous during the course of the dehydrocoupling reaction and for stirring (using a magnetic stir bar) to ultimately cease. It was found that for Rh catalyst loadings greater than 5 mol %, rapid solidification of the reaction mixture occurred at 60 °C and resulting GPC analysis revealed the presence of only oligomeric soluble material. However, for loadings of 1–3 mol %, high molecular weight polymer was generated. This may be due to a smaller number of initiation sites, which would favour the formation of longer chains before monomer was consumed.

In the absence of catalyst, no reaction was detected at 60 °C under the same conditions. In addition, as noted for the formation of the linear dimer **3** and cyclic systems **4a** and **4b** from fluorinated adduct **1**, the dehydrocoupling temperature of 60 °C for the conversion of **2** to **5** in the presence of a Rh catalyst is much lower than that previously reported for the conversions of $PhPH_2{\cdot}BH_3$ to $[PhPH\text{-}BH_2]_n$ (90–130 °C for 6 h) and iBuPH$_2{\cdot}BH_3$ to $[i$BuPH-$BH_2]_n$ (120 °C for 15 h).[16] This demonstrates the significant influence of changing the substituent at phosphorus in the phosphine–borane adduct on the reaction conditions. In particular, this result is important as a high molecular weight polyphosphinoborane **5** can now be accessed at a relatively low temperature. Once again it is likely that the electron-withdrawing p-$CF_3C_6H_4$ group increases the polarity of the P–H bond compared with the unsubstituted Ph substituents, rendering the proton more acidic and therefore more reactive towards dehydrocoupling with the hydridic B–H bonds. With a conven-

ient synthetic route to polyphosphinoborane **5** firmly established, we performed a preliminary investigation into lithographic applications of thin films of this material.

Direct writing of patterned bars by using electron-beam lithography (EBL) and [(*p*-$CF_3C_6H_4$)PH-BH_2]$_n$ 5 as a resist: Patterning is of intense current interest in many areas of science and technology. This has led to the development of a wide variety of fabrication methods that accompany a wide range of available feature sizes.[28,29] For example, techniques employing focused beams of high energy particles such as electrons can be used to generate high resolution patterns in the sub 100 nm range.[30] Furthermore, direct-write EBL is a mask-less lithography in which a processible resist is required. A variety of substances have been shown to act as resists towards EBL including inorganic materials[31,32] and polymers.[33] An example of the latter is poly(methyl methacrylate) (PMMA) which has been used extensively. For instance, monolayer films ranging from one to nine monolayers of PMMA have been shown to act as positive resists by using relatively low electron beam energies.[33]

We decided to explore the use of **5** as a resist towards EBL in an effort to modify the characteristics of the surface. In addition, a thin patterned film of **5** on a Si substrate could yield excellent control over hydrophobic versus hydrophilic surfaces. One would expect that the *p*-CF_3 substituents at phosphorus of **5** would render it relatively hydrophobic. Also, preliminary work in our group has indicated that polyphosphinoboranes are promising preceramic polymers as they can give high ceramic yields upon pyrolysis at 1000 °C.[16] Consequently, we were motivated to extend this to a pre-fabricated design of **5** in order to lay the groundwork for the preparation of patterned boron–phosphide ceramics.

Solutions of **5** in toluene were spin-coated onto silicon substrates affording uniform films. The thickness and refractive index of the films were characterized using ellipsometry and were determined to be 121 ± 2 nm and 1.53, respectively. The refractive index value is very close to the fluoroaryl organic analogue poly(4-trifluoromethylstyrene) which has been determined as 1.50.[34] E-beam lithography was carried out by using a converted thermionic DSM 940 (Zeiss) scanning electron microscope (SEM) with an accelerating voltage of 25 kV and controlled by a Raith ELPHY lithography system. Samples were developed through 1 min sonication in THF prior to characterization. Indeed, resists of **5** were found to act in a negative-tone fashion as the material that was exposed to the e-beam was firmly attached to the substrate while unexposed polymer was removed by sonication. This type of behavior may result from crosslinking of polymer chains via homolytic cleavage of sigma bonds and radical dimerization in the presence of the e-beam rendering them insoluble in organic solvents.

Well-ordered arrays of micron-scale bars about 4.0 μm × 0.7 μm (as determined by SEM) were prepared with a dose of 25 mC cm^{-2} and a beam current of 5.4 nA. They were characterized by using SEM, atomic force microscopy (AFM) and time-of-flight secondary ion mass spectrometry (TOF-SIMS). As can be seen by SEM, the vast majority of the bars are well-formed and intact (Figure 5).

Analysis by AFM over a 20 μm × 20 μm area of bars gave an average height of 113 ± 2 nm and an average width at half height of 1.19 ± 0.02 μm (Figure 6). As can be seen by the cross sectional analysis in Figure 6b, the bars exhibit excellent uniformity both in height and width.

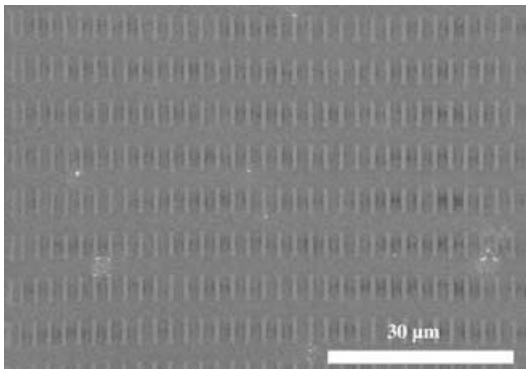

Figure 5. SEM image of bars fashioned by EBL using **5** as a resist.

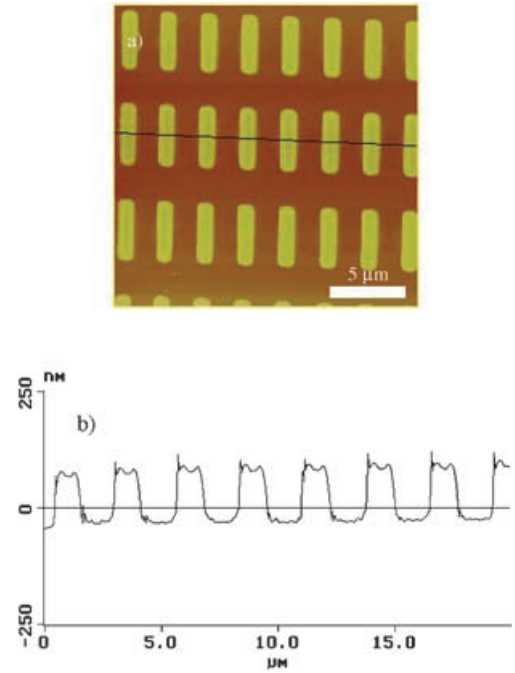

Figure 6. a) Tapping-mode AFM image of lithographically patterned bars of **5** and b) cross-sectional analysis.

The elemental composition of the array of bars was investigated using TOF-SIMS. Boron and fluorine elemental maps over a 40 μm × 40 μm area of the array of bars on the Si substrate were obtained and clearly revealed that boron and fluorine were concentrated within the bars (Figure 7). These results show the promising use of **5** as a resist for EBL. In addition, polyphosphinoboranes are potential precursors to boron-based ceramics.[16] Future work will involve

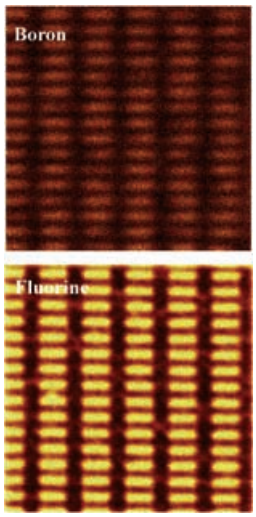

Figure 7. TOF-SIMS elemental maps for B and F of a 40 μm × 40 μm area of bars patterned by EBL using **5** as a resist.

studies of the conversion of micro- and nanopatterned arrays of **5** and related polyphosphinoboranes into ceramic replicas.[32,35,36]

Conclusion

The desire to induce catalytic dehydrocoupling of phosphine–borane adducts under more mild conditions prompted our investigations into the use of electron-withdrawing fluorinated phenyl substituents at phosphorus. We anticipated that the (+)-inductive effect of these substituents on the protons bound to the phosphorus renders them more acidic and therefore more reactive towards dehydrocoupling. This approach was successful, as supported by the Rh catalyzed dehydrocoupling of neat $(p\text{-}CF_3C_6H_4)_2PH{\cdot}BH_3$ **1** at 60 °C to afford the linear dimer $(p\text{-}CF_3C_6H_4)_2PH\text{-}BH_2\text{-}(p\text{-}CF_3C_6H_4)_2P\text{-}BH_3$ (**3**) while at 100 °C, the cyclic species $[(p\text{-}CF_3C_6H_4)_2P\text{-}BH_2]_3$ (**4a**) and $[(p\text{-}CF_3C_6H_4)_2P\text{-}BH_2]_4$ (**4b**) were obtained. The temperatures required for all of these transformations are 20–40 °C less than that of the corresponding dehydrocoupling of $Ph_2PH{\cdot}BH_3$. Analogously, whereas high molecular weight poly(phenylphosphinoborane) is formed upon heating $PhPH_2{\cdot}BH_3$ at 90–130 °C for 6 h in the presence of a small quantity of Rh (pre)catalyst,[15,16] heating $(p\text{-}CF_3C_6H_4)PH_2{\cdot}BH_3$ (**2**) with the same (pre)catalyst at 60 °C for 9 h affords high molecular weight polyphosphinoborane **5**. Lastly, we have shown that thin films of **5** function as negative-tone resists for EBL as well-ordered, patterned arrays of micron-sized bars were generated by the direct-write method. AFM indicated that the bars have excellent structural uniformity while TOF-SIMS confirmed the elemental composition as the boron and fluorine maps proved that these elements were localized within the bars. Future work will involve studies of the pyrolysis of these and related materials in order to prepare patterned boron phosphide ceramics.

Experimental Section

General methods: All reactions were performed under an atmosphere of nitrogen using dry solvents. Workup of all phosphinoborane compounds was carried out in air. PCl_3, $HNEt_2$, $p\text{-}CF_3C_6H_4Br$, *n*BuLi (1.6 M solution in hexanes), HCl (2.0 M solution in diethyl ether), $Li[BH_4]$ (Aldrich) were purchased and used as received. $[\{Rh(\mu\text{-}Cl)(1,5\text{-}cod)\}_2]$[37] was prepared following literature procedures. Hexanes was purified using the Grubbs method.[38] Diethyl ether was dried over Na/benzophenone and distilled prior to use. Pentane, tetrahydrofuran and dichloromethane were ACS grade and used as received from ACP Chemicals Inc. NMR spectra were recorded on a Varian Gemini or Mercury 300 MHz spectrometer. Chemical shifts are referenced to residual protonated solvent resonances (^1H, ^{13}C) or external $BF_3{\cdot}Et_2O$ (^{11}B), $CFCl_3$ (^{19}F) or H_3PO_4 (^{31}P) standards. Mass spectra were obtained with a VG 70–250S mass spectrometer operating in electron impact (EI) mode. The molecular weight of **5** was estimated by gel permeation chromatography (GPC) using a Viscotek GPC MAX liquid chromatograph equipped with a Viscotek Triple Detector Array consisting of a differential refractometer and Ultrastyragel columns with pore sizes of 10^3–10^5 Å. Polystyrene standards were purchased from American Polymer Standards and were used for calibration purposes. A flow rate of 1.0 mL min^{-1} was used, and the eluent was a 3 mM solution of tetra-*n*-butylammonium bromide in THF.

X-ray structural characterization: Diffraction data were collected on a Nonius Kappa-CCD with graphite-monochromated $Mo_{K\alpha}$ radiation (λ = 0.71073 Å). The data were integrated and scaled with the Denzo-SMN package.[39] The structures were solved and refined with the SHELXTL-PC V5.1 software package.[40] Refinement was by full-matrix least-squares on F^2 of all data (negative intensities included). All molecular structures are presented with thermal ellipsoids at a 30% probability level. In all structures, hydrogens bonded to carbon atoms were included in calculated positions and treated as riding atoms. For structures **1**, **2**, **3** and **4b** the hydrogen atoms attached to boron and phosphorus were located and refined with isotropic thermal parameters.

CCDC-258352 (**2**), -258353 (**1**), -258354 (**3**) and -258355 (**4b**) contain the supplementary crystallographic data for this paper. These data can be obtained free of charge from The Cambridge Crystallographic Data Centre via www.ccdc.cam.ac.uk/data_request/cif

Substrate preparation: Silicon (100) substrates were purchased from Wafer World Inc. and cleaned by successive sonication for 10 min in CH_2Cl_2, 2-propanol, piranha solution (30% H_2O_2/concentrated H_2SO_4, 1:3 vol%, **CAUTION**: extremely corrosive!) and deionized water prior to drying in a jet of filtered air.

Spin-coating: $[(p\text{-}CF_3C_6H_4)PH\text{-}BH_2]_n$ (**5**) was dissolved in dry toluene (20 mg mL^{-1}) that was filtered with a Whatman 13 mm GD/X nylon syringe filter (0.45 μm pore size) immediately prior to spin-coating. The ≈2 cm^2 Si wafer was coated with the polymer solution and immediately accelerated to 600 rpm for 18 s followed by an increase to 1000 rpm for 60 s.

Ellipsometry: A Sopra (GES-5) spectroscopic ellipsometer acquired ψ and Δ data from 0.62 to 4.00 eV by using the analyzer in a previous tracking mode and with the integration time for each data point determined by either the minimum threshold of 2000000 detector counts or 10 s. A Levenberg–Marquardt algorithm was used to fit a three-layer model of the sample to the experimentally acquired $\cos(2\psi)/(\sin(2\psi)\cdot\cos(\Delta))$ curves. The three-layer model consisted of a homogeneous crystalline Si substrate with 2 nm of native oxide underneath the polymer layer that was described by a Cauchy dispersion law.

Electron-beam lithography (EBL): The e-beam lithography system was a converted thermionic DSM 940 (Zeiss) scanning electron microscope. The system had been converted by implementing an electrostatic beam blanker and a low hysteresis beam scanning coil. Exposures were carried out at room temperature on a stage without temperature control capabilities in a vacuum of 10^{-5} Torr or better. A remote computer (PC), using a fast IEEE interface drove the beam and the system stage motor through the Raith Elphy-Plus Pattern generator (32 bits architecture). The system stage also had a joystick for manual control and its position was moni-

tored by a laser interferometer (with 5 nm resolution) and read by the computer. A Faraday cup located on the stage connected to a multimeter allowed measurement of the beam current by using the remote computer.

Satisfactory results were obtained by using an accelerating voltage of 25 kV and a current of 5.4 nA with a dose of 25 mC cm^{-2}. The sample was a small silicon wafer (1 cm^2) with a [(*p*-$CF_3C_6H_4$)PH-BH_2]$_n$ (**5**) layer with a thickness of 121 nm. The sample was developed through 1 min sonication in THF. The selected pattern was an array of bars (0.5 μm × 4.0 μm) spaced 2.0 μm apart horizontally and 3.0 μm apart vertically.

Scanning electron microscopy (SEM): SEM images were obtained a Hitachi S-5200 field-emission electron microscope.

Scanning probe microscopy: Tapping mode atomic force microscopy (AFM) was performed on a Digital Instruments Multimode IIIa Nanoscope system using silicon cantilevers with resonant frequencies near 166 kHz. The substrates were mounted on steel sample pucks and imaged in air by using an E-scanner. Image analysis was performed by using the Digital Instruments Nanoscope software. All AFM data sets were collected as 512 × 512 pixel data sets with a scan rate of ca. 1 Hz. Images were processed using Digital Instruments Nanoscope software version 4.42r9 and were flattened using a zero order flatten command. Noise was filtered out using a low-pass filter command.

Time-of-flight secondary ion mass spectrometry (TOF-SIMS): SIMS analysis was carried out with a TOF-SIMS IV instrument (Ion-TOF GmbH, Munster). Surfaces were pre-sputtered with 6 nA Ar^+ (500 eV) over a 300 × 300 μm^2 area while monitoring contaminant signals (polydimethylsiloxane) for the purposes of cleaning. Analysis was performed with a pulsed primary ion beam of focused 25 keV $^{69}Ga^+$ ions incident on the sample at 45°. Boron was mapped by analyzing for the ^{10}B and ^{11}B + ^{10}BH fragments. Fluorine was mapped by analyzing for F^-. High spectral resolution spectra ($m/\Delta m = 10000$) and high spatial resolution images ($\Delta l = 200$ nm) were collected separately. Both high spectral resolution spectra ("bunched mode") and high-spatial-resolution spectra ("burst alignment"-exhibiting unit mass resolution) were collected with a primary ion current of 2.5 pA over a 40 μm × 40 μm area. For both experiments, principal ion dose exceeded the static limit.

(*p*-$CF_3C_6H_4)_2PCl$: Et_2NPCl_2 required for this experiment was prepared according to a literature procedure.[41] *n*Butyllithium (35.4 mL of a 1.6 M solution in hexanes, 56.7 mmol) was slowly added to a solution of *p*-$CF_3C_6H_4Br$ (12.8 g, 56.7 mmol) in diethyl ether (400 mL) at 5 °C. The mixture was stirred for 3 h, and Et_2NPCl_2 (4.93 g, 28.3 mmol) was slowly introduced into the flask at 5 °C. The contents of the flask were brought to room temperature and the mixture was stirred overnight. (*p*-$CF_3C_6H_4)_2PNEt_2$ was not isolated but rather used in situ. $^{31}P\{^1H\}$ NMR (121 MHz, D_2O insert in Et_2O): $\delta = 61.5$.

HCl (35 mL of a 2.0 M solution in diethyl ether, 71 mmol) was added to the reaction mixture containing (*p*-$CF_3C_6H_4)_2PNEt_2$ at −78 °C. The mixture was allowed to warm to room temperature and the solvent was removed in vacuo. The residue was dissolved in hexanes (400 mL) and filtered. The filtrate was concentrated and the remaining residue was distilled (85 °C, 0.001 mmHg) to yield a colorless oil (16.25 g, 80 %). ^1H NMR (300 MHz, C_6D_6): $\delta = 7.17$–7.13 (br m, Ar-H); $^{31}P\{^1H\}$ NMR (121 MHz, C_6D_6): $\delta = 76.7$ (s, (*p*-$CF_3C_6H_4)_2PCl$); ^{19}F NMR (282 MHz, C_6D_6): $\delta = -63.3$ (s, (*p*-$CF_3C_6H_4)_2PCl$).

(*p*-$CF_3C_6H_4)PCl_2$: $(Et_2N)_2PCl$ required for this experiment was prepared according to a literature procedure.[42] *n*Butyllithium (69 mL of a 1.6 M solution in hexanes, 110 mmol) was slowly added to a solution of *p*-$CF_3C_6H_4Br$ (25 g, 110 mmol) in diethyl ether (500 mL) at 5 °C. The mixture was stirred for 1 h and $(Et_2N)_2PCl$ (23.2 g, 110 mmol) was slowly added to the mixture at 5 °C. The contents of the flask were brought to room temperature and the mixture was stirred for 2 h. (*p*-$CF_3C_6H_4)P(NEt_2)_2$ was not isolated but rather used in situ. $^{31}P\{^1H\}$ NMR (121 MHz, D_2O insert in Et_2O): $\delta = 130$.

HCl (275 mL of a 2.0 M solution in diethyl ether, 550 mmol) was added to the reaction mixture containing (*p*-$CF_3C_6H_4)P(NEt_2)_2$ at −78 °C. The mixture was allowed to warm to room temperature and stirred for 12 h. The solvent was removed in vacuo, the solid dissolved in hexanes (500 mL) and then filtered. The filtrate was concentrated and the remaining oil was distilled (85 °C, 11 mmHg) to yield a colorless liquid (20.9 g, 77 %). ^1H NMR (300 MHz, C_6D_6): $\delta = 7.30$ (dd, 2H, $^3J_{PH} = 8.02$ Hz, Ar-H^{para}), 7.10 (d, 2H, $^3J_{HH} = 7.95$ Hz, Ar-H^{meta}); $^{31}P\{^1H\}$ NMR (121 MHz, C_6D_6): $\delta = 157$ (s, (*p*-$CF_3C_6H_4)PCl_2$).

(*p*-$CF_3C_6H_4)_2PH{\cdot}BH_3$ (1): Neat (*p*-$CF_3C_6H_4)_2PCl$ (1.70 g, 4.60 mmol) was added dropwise to a diethyl ether (20 mL) suspension of $LiBH_4$ (0.10 g, 4.80 mmol) cooled to 5 °C with an ice bath. The mixture became cloudy immediately and was allowed to stir for 1 h. The diethyl ether was removed in vacuo, the residue dissolved in hexanes (20 mL) and filtered through Celite. Removal of all volatiles under reduced pressure afforded (*p*-$CF_3C_6H_4)_2PH{\cdot}BH_3$ (**1**) as a colourless oil (1.47 g, 4.37 mmol, 95 %). Single crystals of **1** for X-ray analysis were obtained by cooling the neat compound to −30 °C. ^1H NMR (300 MHz, $CDCl_3$): $\delta = 7.9$–7.7 (m, Ar-H), 6.41 (dm, $^1J_{PH} = 340$ Hz, P*H*), 1.8–0.6 (br m, B*H*); ^{31}P NMR (121 MHz, $CDCl_3$): $\delta = 3.12$ (br d, $^1J_{PH} = 386$ Hz, (*p*-$CF_3C_6H_4)_2PH$); $^{11}B\{^1H\}$ NMR (160 MHz, $CDCl_3$): $\delta = -40.6$ (br, BH_3); EI-MS (70 eV): *m*/*z* (%): 322 (100) [$M^+ - BH_3$].

(*p*-$CF_3C_6H_4)PH_2{\cdot}BH_3$ (2): Neat (*p*-$CF_3C_6H_4)PCl_2$ (1.04 g, 4.21 mmol) was added dropwise to a slurry of $Li[BH_4]$ (182 mg, 8.35 mmol) in diethyl ether (20 mL) at 5 °C. The mixture became cloudy immediately and was stirred for 1.5 h. The solvent was removed in vacuo, the residue re-dissolved in hexanes (20 mL) and then filtered in the presence of Celite. Removal of hexanes under vacuum afforded a colourless oil. Sublimation of this oil overnight at 25 °C under vacuum gave (*p*-$CF_3C_6H_4)PH_2{\cdot}BH_3$ (**2**) as a white solid (0.654 g, 3.41 mmol, 81 %). Single crystals of **2** suitable for X-ray analysis were obtained by cooling the oil to −35 °C. ^1H NMR (300 MHz, $CDCl_3$): $\delta = 7.90$–7.74 (m, Ar-H), 5.60 (dm, 2H, $^1J_{PH} = 370$ Hz, PH_2), 0.91 (br (1:1:1:1) q, 3H, $^1J_{BH} = 104$ Hz, BH_3); ^{31}P NMR (121 MHz, C_6D_6): $\delta = -48.3$ (br t, $^1J_{PH} = 370$ Hz, *P*H_2); $^{11}B\{^1H\}$ NMR (160 MHz, C_6D_6): $\delta = -33.6$ (br d, $^1J_{PB} = 49$ Hz, *B*H_3); ^{11}B NMR (160 MHz, C_6D_6): $\delta = -33.6$ (d of q, $^1J_{BH} = 126$ Hz, *B*H_3); ^{19}F NMR (282 MHz, $CDCl_3$): $\delta = -63.7$ (s, C*F*$_3$); EI-MS (70 eV): *m*/*z* (%): 178 (100) [$M^+ - BH_3$].

(*p*-$CF_3C_6H_4)_2PH{\cdot}BH_2$-(*p*-$CF_3C_6H_4)_2P{\cdot}BH_3$ (3): Neat **1** (0.60 g, 1.79 mmol) and [{Rh(μ-Cl)(1,5-cod)}$_2$] (ca. 10 mg, 2 mol % Rh) were stirred at 90 °C for 14 h. During this period the orange solution gradually solidified. Recrystallization from diethyl ether gave colourless crystals of **3** (0.828 g, 1.24 mmol, 69 %), which were suitable for single crystal X-ray analysis. M.p. 155–157 °C; ^1H NMR (400 MHz, $CDCl_3$): $\delta = 7.74$–7.45 (m, aromatic), 6.98 (dm, $^1J_{PH} = 425$ Hz, PH), 1.9–2.8 (br, BH_2), 1.5–0.5 (br, BH_3); $^{31}P\{^1H\}$ NMR (121 MHz, $CDCl_3$): $\delta = -2.13$ (br, (*p*-$CF_3C_6H_4)_2PH$), −14.7 (br, (*p*-$CF_3C_6H_4)_2P$); ^{31}P NMR (121 MHz, $CDCl_3$): $\delta = -2.13$ (br d, $^1J_{PH} = 437$ Hz, (*p*-$CF_3C_6H_4)_2PH$); $^{11}B\{^1H\}$ NMR (160 MHz, $CDCl_3$): $\delta = -33.6$ (br, BH_2), −37.8 (br, BH_3); ^{19}F NMR (282 MHz, $CDCl_3$): $\delta = -63.6$ (s, (*p*-$CF_3C_6H_4)_2P{\cdot}BH_3$), −64.0 (s, (*p*-$CF_3C_6H_4)_2PH$); EI-MS (70 eV): *m*/*z* (%): 656 (21) [$M^+ - BH_3$], 127 (100) [$C_6H_4CF_2^+$].

Catalytic dehydrocoupling of (*p*-$CF_3C_6H_4)_2PH{\cdot}BH_3$ at 100 °C: Neat **1** (0.41 g, 1.22 mmol) and [{Rh(μ-Cl)(1,5-cod)}$_2$] (4 mg, ca. 1 mol % Rh) were heated at 100 °C for 15 h, and the resulting solid material was purified and analyzed as mentioned below.

[(*p*-$CF_3C_6H_4)_2P{\cdot}BH_2]_3$ (4a): Dichloromethane (5 mL) was added to the above reaction mixture and the suspension was filtered followed by solvent removal giving **4a** as a light yellow solid (0.978 g, 0.976 mmol, 80 %). M.p. 206–210 °C; ^1H NMR (300 MHz, [D_8]THF): $\delta = 7.8$–7.6 (br m, Ar-H^{meta}), 7.53 (d, $^3J_{HH} = 8.1$ Hz, Ar-H^{ortho}), 2.5–1.8 (br, BH_2); $^{31}P\{^1H\}$ NMR (121 MHz, $CDCl_3$): $\delta = -18.1$; $^{11}B\{^1H\}$ NMR (160 MHz, $CDCl_3$): $\delta = -33.7$ (br, BH_2); EI-MS (70 eV): *m*/*z* (%): 681 (100) [$M^+ - $(*p*-$CF_3C_6H_4)_2P$].

[(*p*-$CF_3C_6H_4)_2P{\cdot}BH_2]_4$ (4b): To a mixture containing [(*p*-$CF_3C_6H_4)_2P{\cdot}BH_2]_3$ and [(*p*-$CF_3C_6H_4)_2P{\cdot}BH_2]_4$, prepared by the above procedure, was added CH_2Cl_2 (≈10 mL) and the mixture stirred for 10 min. The suspension was filtered and a colourless solid was collected (0.326 g, 0.244 mmol, 20 %). Single crystals of **4b** for X-ray analysis were obtained from the slow evaporation of a THF solution. M.p. 260 °C (decomp); ^1H NMR (300 MHz, [D_8]THF): $\delta = 7.56$–7.48 (br m, Ar-H^{meta}), 7.30 (d, $^3J_{HH} = 8.1$ Hz, Ar-H^{ortho}), 3.2–2.2 (br, BH_2); $^{31}P\{^1H\}$ NMR (121 MHz, $CDCl_3$): $\delta = -17.8$; $^{11}B\{^1H\}$ NMR (160 MHz, $CDCl_3$): $\delta = -31.3$ (br, BH_2); EI-MS (70 eV): *m*/*z* (%): 1334 (19) [M^+], 300 (100) [$PC_6H_3CF_3$-$(C_6H_3CF_2)^+$].

High molecular weight $[(p\text{-}CF_3C_6H_4)PH{\cdot}BH_2]_n$ (5): In a typical experiment, neat (p-$CF_3C_6H_4$)$PH_2{\cdot}BH_3$ (**2**) (0.155 g, 0.81 mmol) and [{Rh(μ-Cl)-(1,5-cod)}$_2$] (ca. 0.010 g, 2.5 mol% Rh) were stirred for 9 h at 60°C, gas evolution was observed and the contents of the flask slowly solidified. After cooling to room temperature, the resulting dark yellow solid was dissolved in THF (1 mL), filtered to remove residual catalyst and precipitated into pentane (ca. 150 mL). The light brown fibrous product **5** was dried under vacuum at 25°C for 18–24 h and isolated (0.109 g, 0.567 mmol, 70%). GPC analysis (3 mM solution of $[Bu_4N]Br$ in THF, polystyrene standards): $M_w = 56170$, PDI = 1.67; ^{1}H NMR (300 MHz, $CDCl_3$): δ = 7.9–6.5 (br, Ar-*H*), 4.42 (br d, $^1J_{PH} = 354$ Hz, P*H*), 2.2–0.8 (br, BH_2); ^{11}B{^{1}H} NMR (160 MHz, $CDCl_3$): $\delta = -34.3$ (br, BH_2); ^{31}P{^{1}H} NMR (121 MHz, $CDCl_3$): $\delta = -46.9$ (t); ^{19}F NMR (282 MHz, $CDCl_3$): $\delta = -62.5$ (s, CF_3).

No reaction was detected by ^{31}P NMR when neat **2** was heated at 60°C for 9 h. However, approximately 20% conversion to polyphosphinoborane **5** was observed when neat **2** was heated at 75°C for 9 h.

Acknowledgements

T.J.C. is grateful for a University of Toronto Open Fellowship, S.B.C. thanks NSERC for a PDF and I.M. thanks the Canadian government for a Canada Research Chair. We thank David Rider and Kun Liu for help with AFM, Chantal Paquet for ellipsometry measurements, Alex Bartole-Scott for GPC measurements and Dr. Hendrik Dorn and Dr. Eric Rivard for helpful discussions.

[1] F. Gauvin, J. F. Harrod, H.-G. Woo, *Adv. Organomet. Chem.* **1998**, *42*, 363.
[2] J. A. Reichl, D. H. Berry, *Adv. Organomet. Chem.* **1998**, *43*, 197.
[3] C. A. Jaska, A. Bartole-Scott, I. Manners, *Dalton Trans.* **2003**, 4015.
[4] C. T. Aitken, J. F. Harrod, E. Samuel, *J. Am. Chem. Soc.* **1986**, *108*, 4059.
[5] T. Imori, V. Lu, H. Cai, T. D. Tilley, *J. Am. Chem. Soc.* **1995**, *117*, 9931.
[6] a) A. J. Hoskin, D. W. Stephan, *Angew. Chem.* **2001**, *113*, 1917; *Angew. Chem. Int. Ed.* **2001**, *40*, 1865; b) V. P. W. Böhm, M. Brookhart, *Angew. Chem.* **2001**, *113*, 4832; *Angew. Chem. Int. Ed.* **2001**, *40*, 4694.
[7] Q. Jiang, P. J. Carroll, D. H. Berry, *Organometallics* **1993**, *12*, 177.
[8] J. M. Fischer, W. E. Piers, S. D. P. Batchilder, M. J. Zaworotko, *J. Am. Chem. Soc.* **1996**, *118*, 283.
[9] R. Shu, L. Hao, J. F. Harrod, H.-G. Woo, E. Samuel, *J. Am. Chem. Soc.* **1998**, *120*, 12988.
[10] J. He, H. Q. Liu, J. F. Harrod, R. Hynes, *Organometallics* **1994**, *13*, 336.
[11] a) Y. Li, Y. Kawakami, *Macromolecules* **1999**, *32*, 6871; b) R. Zhang, J. E. Mark, A. R. Pinhas, *Macromolecules* **2000**, *33*, 3508; c) T. E. Ready, B. P. S. Chauhan, P. Boudjouk, *Macromol. Rapid Commun.* **2001**, *22*, 654.
[12] Recently, the ambient temperature dehydrocoupling of P-H and Al/Ga–H bonds to form Lewis acid/base stabilized phosphine-alanes and gallanes has been reported, see: U. Vogel, A. Y. Timoshkin, M. Scheer, *Angew. Chem.* **2001**, *113*, 4541; *Angew. Chem. Int. Ed.* **2001**, *40*, 4409.
[13] For recent work from other groups on the formation of new inorganic polymers based on phosphorus or boron see a) N. Matsumi, K. Naka, Y. Chujo, *J. Am. Chem. Soc.* **1998**, *120*, 5112; b) V. A. Wright, D. P. Gates, *Angew. Chem.* **2002**, *114*, 2495; *Angew. Chem. Int. Ed.* **2002**, *41*, 2389; c) C.-W. Tsang, M. Yam, D. P. Gates, *J. Am. Chem. Soc.* **2003**, *125*, 1480; d) R. C. Smith, J. D. Protasiewicz, *J. Am. Chem. Soc.* **2004**, *126*, 2268; e) T. J. Peckham, J. A. Massey, C. H. Honeyman, I. Manners, *Macromolecules* **1999**, *32*, 2830; f) M. Grosche, E. Herdtweck, F. Peters, M. Wagner, *Organometallics* **1999**, *18*, 4669; g) Y. Qin, C. Pagba, P. Piotrowiak, F. Jäkle, *J. Am. Chem. Soc.* **2004**, *126*, 7015; h) T. Baumgartner, T. Neumann, B. Wirges, *Angew. Chem.* **2004**, *116*, 6323; *Angew. Chem. Int. Ed.* **2004**, *43*, 6197.
[14] H. Dorn, R. A. Singh, J. A. Massey, A. J. Lough, I. Manners, *Angew. Chem.* **1999**, *111*, 3540; *Angew. Chem. Int. Ed.* **1999**, *38*, 3321.
[15] H. Dorn, R. A. Singh, J. A. Massey, J. M. Nelson, C. A. Jaska, A. J. Lough, I. Manners, *J. Am. Chem. Soc.* **2000**, *122*, 6669.
[16] H. Dorn, J. M. Rodezno, B. Brunnhöfer, E. Rivard, J. A. Massey, I. Manners, *Macromolecules* **2003**, *36*, 291.
[17] For recent theoretical work on polyphosphinoboranes see: a) D. Jacquemin, C. Lambert, E. A. Perpète, *Macromolecules* **2004**, *37*, 1009; b) D. Jacquemin, V. Wathelet, E. A. Perpète, *Macromolecules* **2004**, *37*, 5040.
[18] a) C. A. Jaska, K. Temple, A. J. Lough, I. Manners, *J. Am. Chem. Soc.* **2003**, *125*, 9424; b) C. A. Jaska, I. Manners, *J. Am. Chem. Soc.* **2004**, *126*, 1334; c) C. A. Jaska, I. Manners, *J. Am. Chem. Soc.* **2004**, *126*, 9776.
[19] H. Dorn, E. Vejzovic, A. J. Lough, I. Manners, *Inorg. Chem.* **2001**, *40*, 4327.
[20] J. Scheirs, *Modern Fluoropolymers: High Performance Polymers for Diverse Applications*, Wiley, New York, **1997**.
[21] K. Bourumeau, A.-C. Gaumont, J.-M. Denis, *J. Organomet. Chem.* **1997**, *529*, 205.
[22] J. C. Huffman, W. A. Skupinski, K. G. Caulton, *Cryst. Struct. Commun.* **1982**, *11*, 1435.
[23] W. T. Klooster, T. F. Koetzle, P. E. M. Siegbahn, T. B. Richardson, R. H. Crabtree, *J. Am. Chem. Soc.* **1999**, *121*, 6337.
[24] P. S. Bryan, R. L. Kuczkowski, *Inorg. Chem.* **1972**, *11*, 553.
[25] We have previously observed this phenomenon in the ^{29}Si NMR spectrum of a polyferrocenylsilane $[Fe(\eta\text{-}C_5H_4)_2SiRR']_n$ where R = Me and R′ = Cl see: D. L. Zechel, K. C. Hultzsch, R. Rulkens, D. Balaishis, Y. Ni, J. K. Pudelski, A. J. Lough, I. Manners, D. A. Foucher, *Organometallics* **1996**, *15*, 1972. For a general overview of dyad resolution using NMR spectroscopy see: F. Heatley in *NMR Spectroscopy of Polymers* (Ed.: R. N. Ibbett), Blackie, London, **1993**, pp. 1–49.
[26] H. Nöth, B. Wrackmeyer, *Nuclear Magnetic Resonance Spectroscopy of Boron Compounds*, Springer, Berlin, **1978**.
[27] Previous reports have mentioned similar problems with the GPC analysis of polyphosphazenes that were circumvented by the addition of a small amount (ca. 0.1 wt%) of $[Bu_4N]Br$ to the THF mobile phase, see: T. H. Mourey, S. M. Miller, W. T. Ferrar, T. R. Molaire, *Macromolecules* **1989**, *22*, 4286.
[28] Y. Xia, G. M. Whitesides, *Angew. Chem.* **1998**, *110*, 568; *Angew. Chem. Int. Ed. Engl.* **1998**, *37*, 550.
[29] M. Geissler, Y. Xia, *Adv. Mater.* **2004**, *16*, 1249.
[30] G. R. Brewer, *Electron-Beam Technology in Microelectronic Fabrication*, Academic Press, New York, **1980**.
[31] J. Fujita, H. Watanabe, Y. Ochiai, S. Manako, J. S. Tsai, S. Matsui, *Appl. Phys. Lett.* **1995**, *66*, 3064.
[32] S. B. Clendenning, S. Aouba, M. S. Rayat, D. Grozea, J. B. Sorge, P. M. Brodersen, R. N. S. Sodhi, Z.-H. Lu, C. M. Yip, M. R. Freeman, H. E. Ruda, I. Manners, *Adv. Mater.* **2004**, *16*, 215.
[33] S. W. J. Kuan, C. W. Franck, Y. H. Y. Lee, T. Eimori, D. R. Allee, R. F. W. Pease, R. Browning, *J. Vac. Sci. Technol. B* **1989**, *7*, 1745.
[34] B. Bömer, H. Hagemann, *Angew. Makromol. Chem.* **1982**, *109*, 285.
[35] U. P. Schönholzer, N. Stutzmann, T. A. Tervoort, P. Smith, L. J. Gauckler, *J. Am. Ceram. Soc.* **2002**, *85*, 1885.
[36] S.-J. Kim, D. E. McKean, *J. Mater. Sci. Lett.* **1998**, *17*, 141.
[37] G. Giordano, R. H. Crabtree, *Inorg. Synth.* **1979**, *19*, 218.
[38] A. B. Pangborn, M. A. Giardello, R. H. Grubbs, R. K. Rosen, F. J. Timmers, *Organometallics* **1996**, *15*, 1518.
[39] Z. Otwinowski, W. Minor, *Methods Enzymol.* **1997**, *276*, 307.
[40] G. M. Sheldrick, SHELXTL-PC V5.1, Bruker Analytical X-Ray Systems Inc., Madison, WI, **1997**.
[41] R. B. King, N. D. Sadanani, *Synth. React. Inorg. Met.-Org. Chem.* **1985**, *15*, 149.
[42] R. B. King, P. M. Sundaram, *J. Org. Chem.* **1984**, *49*, 1784.

Received: December 16, 2004
Published online: May 18, 2005